Saturated Fat is More Metabolically Harmful for the Human Liver than Unsaturated Fat or Simple Sugars

Short title: Diets and the liver fat

Panu K. Luukkonen[1,2], Sanja Sädevirta[1,2], You Zhou[1,3], Brandon Kayser[4], Ashfaq Ali[5], Linda Ahonen[5], Susanna Lallukka[1,2], Véronique Pelloux[4], Melania Gaggini[6], Ching Jian[7], Antti Hakkarainen[8], Nina Lundbom[8], Helena Gylling[2], Anne Salonen[7], Matej Orešič[5,9,10], Tuulia Hyötyläinen[5,11], Marju Orho-Melander[12], Aila Rissanen[13], Amalia Gastaldelli[6], Karine Clément[4,14], Leanne Hodson[15], Hannele Yki-Järvinen[1,2,16]

[1]Minerva Foundation Institute for Medical Research, Helsinki, Finland; [2]Department of Medicine, University of Helsinki and Helsinki University Central Hospital, Helsinki, Finland; [3]Systems Immunity University Research Institute and Division of Infection and Immunity, School of Medicine, Cardiff University, Cardiff, United Kingdom; [4]Sorbonne Universités, INSERM, UMRS 1166, Nutriomics team, ICAN, F-75013, Paris, France; [5]Steno Diabetes Center, Gentofte, Denmark; [6]Institute of Clinical Physiology, CNR, Pisa, Italy; [7]Immunobiology Research Program, Department of Bacteriology and Immunology, University of Helsinki; [8]Helsinki Medical Imaging Centre, Radiology, Helsinki University Hospital and University of Helsinki; [9]School of Medical Sciences, Örebro University, Örebro, Sweden; [10]Turku Centre for Biotechnology, University of Turku and Åbo Akademi University, Turku, Finland; [11]Department of Chemistry, Örebro University, Örebro, Sweden; [12]Lund University, Malmö, Sweden; [13]Obesity Research Unit, Department of Psychiatry, Helsinki University Central Hospital; [14]Assistance Publique-Hôpitaux de Paris (AP-HP), Pitié-Salpêtrière Hospital, Nutrition Department F-75013, Paris, France; [15]Oxford Centre for Diabetes, Endocrinology and Metabolism, University of Oxford, Oxford, UK; [16]Corresponding Author

Address correspondence to: Hannele Yki-Järvinen, MD; Biomedicum Helsinki, Haartmaninkatu

8, Room C425B, FIN - 00290 Helsinki, Finland; Phone: +358 50 427 1664; E-mail:

Hannele.Yki-Jarvinen@helsinki.fi

Word count: 3989

Number of Tables: 1

Number of Figures: 3

ABSTRACT

OBJECTIVE. NAFLD, i.e. increased intrahepatic triglycerides (IHTG), predisposes to type 2 diabetes and cardiovascular disease. Adipose tissue lipolysis and hepatic *de novo* lipogenesis (DNL) are the main pathways contributing to IHTG. We hypothesized that dietary macronutrient composition influences the pathways, mediators and magnitude of weight gain-induced changes in IHTG..

RESEARCH DESIGN AND METHODS. We overfed 38 overweight subjects (age 48±2, BMI 31±1 kg/m^2, liver fat 4.7±0.9%) 1000 extra kilocalories/day of either saturated (SAT) or unsaturated (UNSAT) fat or simple sugars (CARB) for 3 weeks. We measured IHTG (^{1}H-MRS), pathways contributing to IHTG (lipolysis ([^{2}H$_5$]glycerol) and DNL (^{2}H$_2$O) basally and during euglycemic hyperinsulinemia), insulin resistance, endotoxemia, plasma ceramides and adipose tissue gene expression at 0 and 3 weeks.

RESULTS. Overfeeding SAT increased IHTG more (+55%) than UNSAT (+15%, p<0.05). CARB increased IHTG (+33%) by stimulating DNL (+98%). SAT significantly increased whilst UNSAT decreased lipolysis. SAT induced insulin resistance, endotoxemia and significantly increased multiple plasma ceramides. The diets had distinct effects on adipose tissue gene expression.

CONCLUSIONS. Macronutrient composition of excess energy influences pathways of IHTG: CARB increases DNL, whilst SAT increases and UNSAT decreases lipolysis. SAT induced greatest increase in IHTG, insulin resistance and harmful ceramides. Decreased intakes of SAT could be beneficial in reducing IHTG and the associated risk of diabetes.

INTRODUCTION

The rapid increase in the prevalence of obesity has led to a co-epidemic of non-alcoholic fatty liver disease (NAFLD) (1). NAFLD is strongly associated with insulin resistance (IR) and predicts the development of type 2 diabetes and cardiovascular disease (CVD) (1). Whilst obesity is its primary acquired cause, some subjects who gain weight do not develop NAFLD (1,2). Whether composition of the diet contributes to susceptibility of NAFLD is unclear. Saturated but not polyunsaturated fat has been reported to increase intrahepatic triglycerides (IHTG) in young non-obese adults, despite similar weight gain (2). The epidemic of obesity has been attributed to an increased intake of simple sugars (3). However, there are no studies comparing the effects of overfeeding simple sugars, saturated or unsaturated fat diets on IHTG.

Fatty acids (FAs) in IHTG can originate from adipose tissue lipolysis, hepatic *de novo* lipogenesis (DNL) and dietary fat (4). Lipolysis provides most of the FAs used for synthesis of IHTG (4). DNL produces exclusively saturated fatty acids (SFA) from substrates such as simple sugars (4,5). Excess sugar intakes increase DNL and IHTG content in humans (5). In mice, a high-fat diet increases adipose tissue lipolysis (6). The pathway *via* which IHTG are synthesized in response to overconsuming fat has not been studied in humans.

While IHTG are commonly associated with IR, triglycerides (TG) themselves are inert and do not confer IR (7). We have previously shown in humans that IR co-segregates with hepatic ceramides, independent of IHTG and obesity (7). Ceramides are synthesized *de novo* from SFA such as palmitate, and interfere glucose metabolism by inhibiting insulin signaling (8) and by stimulating hepatic gluconeogenesis (9). Inflammatory mediators such as endotoxins derived from gut bacteria may induce IR by upregulating ceramide synthesis (10). In mice, saturated but not unsaturated fat feeding increases the proportion of endotoxin-containing bacteria in the gut, plasma concentrations of endotoxin, and induces IR (11,12). To our knowledge, there are no

human data comparing the effects of hypercaloric diets enriched with either saturated or unsaturated fat or simple sugars on IR, plasma ceramides, endotoxemia and gut microbiota.

In the present study, we hypothesized that the metabolic effects of a hypercaloric diet depend on the macronutrient composition. Specifically, we hypothesized that (a) overconsumption of simple sugars stimulates DNL whilst saturated fat increases lipolysis, (b) overconsumption of simple sugars and saturated fat increases availability of SFA and thereby ceramide synthesis, (c) saturated but not unsaturated fat or simple sugar diets induce endotoxemia which may further increase ceramide synthesis. Accordingly, we compared the effects of three hypercaloric (1000 extra kilocalories/day for 3 weeks) diets on (i) IHTG content, (ii) rates of DNL, (iii) rates of lipolysis, (iv) adipose tissue transcriptome, (v) plasma concentrations of ceramides, (vi) gut microbiota and a circulating marker of endotoxemia **(Figure 1A)**.

RESEARCH DESIGN AND METHODS

Subjects. Subjects in this study (ClinicalTrials.gov, NCT02133144) were recruited by newspaper advertisements or by contacting subjects who previously had participated in metabolic studies. Exclusion criteria included i) type 1 or 2 diabetes, ii) pre-existing autoimmune, viral or drug-induced liver disease, iii) excessive use of alcohol (over 20g/day for women and over 30g/day for men), iv) evidence of any other acute or chronic disease, v) extreme obesity (BMI≥40 kg/m^2), vi) use of drugs influencing glucose or lipid metabolism, vii) pregnancy or lactation. All subjects suitable for the study based on a telephone interview were invited for a screening visit. The flow chart of study subjects is shown in **Figure S1**. The nature and potential risks of the study were explained to volunteers prior to obtaining written informed consent. The ethics committee of the Helsinki University Hospital approved the study protocol.

*Study design (**Figure 1A**)*. The day before the metabolic study, a blood sample was taken for measurement of background enrichment of ^{2}H in plasma water and VLDL-TG palmitate for measurement of DNL. Subjects then underwent measurement of IHTG by proton magnetic resonance spectroscopy (^{1}H-MRS). The following morning subjects arrived at the clinical research unit after an overnight fast and after consuming deuterated water (^{2}H$_2$O) (3 g/kg body water) the evening prior to the study day, to achieve a plasma water enrichment of 0.3% for the measurement of DNL. Fecal samples were self-collected and stored immediately at −20°C and within 24 h at -80°C until analysis. Body composition (InBody 720, Biospace, Seoul, Korea), weight and height were measured and blood samples taken for measurement of DNL and for liver function tests, fasting glucose, FFA, insulin, total, HDL and LDL cholesterol and TG concentrations. Thereafter, a euglycemic hyperinsulinemic clamp combined with infusion of [^{2}H$_5$]glycerol for measurement of lipolysis was performed.

After the baseline visit, the subjects were randomized to one of three groups to consume a hypercaloric (1000 excess kcal/day) diet for 3 weeks with excess energy originating predominantly from either saturated fat (SAT, 76% from SFA, 21% from MUFA and 3% from PUFA), unsaturated fat (UNSAT, 57% from monounsaturated fatty acids (MUFA), 22% from polyunsaturated fatty acids (PUFA), 21% from saturated fatty acids (SFA)), or from simple sugars (CARB, 100% simple sugars). The overfeeding diets were provided to participants, and consisted in the SAT group of 30g coconut oil, 40g butter and 100g of 40% fat containing blue cheese as extra energy per day, in the UNSAT group of 36g olive oil, 26g pesto, 54g pecan nuts and 20g of butter, and in the CARB group of 2.8dL orange juice, 4.3dL of a sugar-sweetened beverage, and 200g of candy. Of the overfeeding energy, 2%, 91% and 7% came from carbohydrate, fat and protein in the UNSAT group and 1%, 86% and 13% from these sources in the SAT group, respectively and 100% from simple sugars in the CARB group. After 3 weeks of consuming the hypercaloric diets, baseline measurements were repeated.

Adherence to the diets was reinforced by weekly contacts with the study dietician, and verified by 3-day dietary records, which were performed before and after 3 weeks on the diet, and by measuring the FA composition of fasting VLDL-TG as an objective biomarker of recent dietary FA intake (13). The food records were analyzed using the AivoDiet software (version 2.0.2.3, Aivo Finland, Turku, Finland).

Methods. The FA composition of VLDL-TG was assessed as described in Supplementary Material. Respiratory gas exchange and rates of resting energy expenditure and substrate oxidation were recorded by indirect calorimetry as described (14). IHTG content was determined by ^{1}H-MRS and visceral and subcutaneous fat by magnetic resonance imaging using 1.5T Siemens Avanto^{fit} as described (5). Fasting DNL was assessed based on the incorporation of deuterium from ^{2}H$_2$O in plasma water (Finnigan GasBench-II, ThermoFisher Scientific, UK) into VLDL-

TG palmitate using gas chromatography/mass spectrometry (GC/MS). Further details of DNL methodology are given in Supplementary Material. Insulin action on serum FFA and glycerol rate of appearance (R_a) were determined using the euglycemic hyperinsulinemic clamp technique as previously described (5). The duration of the insulin infusion was 120 min (120-240 min) and rate of the continuous insulin infusion was 0.4 mU/kg·min. Adipose tissue transcriptome and gut microbiota were analyzed as detailed in Supplement Material. Plasma ceramide analyses were performed as described (15). Serum lipopolysaccharide-binding protein (LBP) and soluble cluster of differentiation 14 (sCD14) were measured by quantitative enzyme-linked immunosorbent assay using human LBP DuoSet® and human CD14 DuoSet® kits (R&D Systems, Minneapolis, MN, USA). Plasma adiponectin (7) and other analytical procedures were assessed as described (15)

Power calculation. IHTG was the primary outcome. Based on a previous study (2), 12 subjects per group were needed to detect a 1.4% difference in change in liver fat between the three groups with an alpha of 0.05, beta of 0.2 and standard deviation of 1.0.

Statistics. Continuous variables were tested for normality using the Kolmogorov-Smirnov method. Changes between groups were compared using one-way analysis of variance followed by a Fisher's least significant differences test to analyze the differences between groups. Nonparametric variables were log-transformed for analysis and back-transformed for presentation, or analyzed nonparametrically with the Kruskal-Wallis test. The paired Student's t-test was used to explore within-group effects of overfeeding. Categorical variables were analyzed with Fisher's exact test. Data are presented as the means with SDs for normally distributed variables and as medians (quartiles 1-3) for non-normally distributed variables unless otherwise specified. $P < 0.05$ were considered statistically significant.

RESULTS

Baseline characteristics

Baseline studies were performed in 39 subjects, of which 38 completed the study. The SAT, UNSAT and CARB groups were comparable with respect to age, gender, BMI, IHTG, body composition and biochemical characteristics such as glucose, insulin, lipids and liver enzymes (**Table 1**). Baseline composition of the diet (**Table S1**) and the FA composition of VLDL-TG (**Table S2**) were also comparable between the groups.

Compliance

Macronutrient composition. At the end of the overfeeding period, fat comprised 60 [54–64] and 59 [53–61]% of total energy intake in the SAT and UNSAT groups, respectively. These percentages were 2-fold higher than in the CARB group (24 [20–26]%, **Table S1**). Saturated fat intake was 2-fold higher in the SAT (33 [28–36]%) than the UNSAT (14 [14–18]% group (p<0.001). Monounsaturated (28 [23–30] vs. 13 [12–15]%, UNSAT vs. SAT, p<0.001) and polyunsaturated (11 [10–14] vs. 5 [4–5]%, respectively, p<0.001) fat intakes were 2-fold higher in the UNSAT than the SAT group. The % total energy intake from carbohydrate was 2.8-fold higher in the CARB (64 [58–68]%) than in the UNSAT (23 [19–29]%, p<0.001) or the SAT (26 [23–32]%, p<0.001) group.

FA composition of VLDL-TG. The FA composition of fasting plasma VLDL-TG, was used to monitor compliance (**Figure 1B**). During the SAT diet, the abundance of SFA in VLDL-TG increased significantly: 16:0 by 17% (26.2±3.6 vs. 30.7±3.6 mol% (p<0.001)), 18:0 (3.1±1.2 vs. 4.1±1.2 mol% (p<0.01)) and 14:0 (1.8±0.7 vs. 4.8±1.7 mol% (p<0.001)). The abundance of 18:2 decreased significantly during the SAT diet. During the UNSAT diet, 18:2 increased significantly (p<0.01). During the CARB diet, the abundance of 16:0, 14:0 and 16:1 increased and 18:2 decreased significantly (p<0.05) (**Figure 1B**).

Body weight and composition

In all subjects, body weight increased by 1.4±1.5 % from 92.1±17.0 to 93.3±17.2 kg (p<0.001). Changes in body weight averaged 1.4±1.2 kg in the SAT, 0.9±1.1 kg in the UNSAT and 1.4±1.6 kg in the CARB groups (p=NS). Visceral (1940±1605 vs. 2072±1674 cm^3; 2019±1328 vs. 2080±1361 cm^3; 2014±1217 vs. 2115±1351 cm^3, before vs. after, respectively in the SAT, UNSAT and CARB groups) and subcutaneous (4770±2152 vs. 4906±2090 cm^3; 4732±2350 vs. 4805±2473 cm^3; 5133±2154 vs. 5204±2157 cm^3, respectively) fat volumes tended to increase but did not change significantly during overfeeding.

Energy expenditure and substrate oxidation rates

All subjects. As expected, overfeeding increased resting energy expenditure significantly from 7.49±1.36 to 7.61±1.48 MJ/day (p<0.05) in all subjects. Rates of energy expenditure and substrate oxidation rates expressed per kg body weight or fat free mass remained unchanged in all subjects, within and between groups (data not shown). Non-protein respiratory quotient (NPRQ) did not change with overfeeding (data not shown).

Intrahepatic triglycerides

IHTG increased by 55% (4.9±6.6 vs. 7.6±8.8% (p<0.001)) in the SAT group, by 15% (4.8±4.9 vs. 5.5±4.8% (p<0.02)) in the UNSAT group, and by 33% (4.3±4.7 vs. 5.7±5.4% (p<0.02)) in the CARB group (**Figure 1C**). The increase was significantly greater in the SAT than the UNSAT (p<0.01) group (**Figure 1D**). This difference was independent of changes in body weight as determined by the significantly different intercepts of the linear regression lines between change in IHTG and change in body weight in the SAT vs. the UNSAT group (p<0.05, **Figure S2**).

***De novo* lipogenesis**

Hepatic DNL, as determined by the amount of newly synthesized palmitate in VLDL-TG, increased significantly during the CARB diet (96 [47–116] vs. 190 [61–303] µmol/L, p<0.05) but not other diets (**Figure 2A**).

Lipolysis

Basal state. Fasting serum insulin increased significantly with overfeeding in the SAT group (8.1 [5.8–11.9] vs. 9.5 [5.9–11.9] mU/L, p<0.05) but remained unchanged in the UNSAT (9.1 [6.5–14.6] vs. 9.5 [7.8–11.1] mU/L, NS) and CARB (10.3 [6.2–19.2] vs. 11.1 [6.9–23.8] mU/L, NS) groups. Basal whole-body glycerol R_a remained unchanged in all groups (**Figure 2B**).

Euglycemic hyperinsulinemia. During hyperinsulinemia, increases in serum insulin concentrations were similar before and after the diets (22±7 vs. 22±6 mU/L, p=NS) with no differences between the SAT, UNSAT and CARB groups (data not shown). Whole-body glycerol R_a during euglycemic hyperinsulinemia compared to baseline increased in SAT (2.08±0.46 vs. 2.31±0.59 µmol/kg·min, p<0.05), decreased in the UNSAT (2.59±0.87 vs. 2.14±0.77 µmol/kg·min, p<0.05), and remained unchanged in the CARB (2.15±0.74 vs. 2.27±0.64 µmol/kg·min, NS) group after overfeeding (**Figure 2C**). Insulin-induced suppression of whole-body glycerol R_a increased significantly more in the SAT compared to the UNSAT (p<0.001) and the CARB compared to the UNSAT (p<0.01) group (**Figure 2C**).

Serum FFA. Serum FFA concentrations, which reflect the net effects of lipolysis and lipogenesis, remained unchanged in the SAT group but decreased significantly during hyperinsulinemia by overfeeding in the UNSAT and CARB groups (**Figure S3**).

Adipose tissue transcriptome

Gene set analysis identified 28 reporter pathways out of 134 curated KEGG pathways at a 5% FDR. The SAT and CARB diets changed 18, while the UNSAT diet changed 5 pathways, which were highly distinctive between the diets. Only 3 pathways overlapped between all diets (**Figure 2D**). The pathways upregulated by the SAT diet included those related to inflammation, such as genes related to E. coli infection, natural killer cell-mediated cytotoxicity, NOD-like receptor signaling and leukocyte transendothelial migration, and to glycerolipid metabolism. The SAT and CARB diets shared some pathways related to inflammation, such as genes related to antigen processing, chemokine signaling, and hematopoietic cell lineage. In addition, CARB induced pathways related to carbohydrate metabolism such as fructose and mannose metabolism, pentose phosphate pathway and glycolysis/gluconeogenesis. The UNSAT diet upregulated pathways related to oxidative phosphorylation and extracellular matrix.

Insulin resistance and plasma ceramides

In the SAT group, HOMA-IR increased significantly by 23% (1.9 [1.3–3.2] vs. 2.2 [1.4–3.3], $p<0.05$). In addition, total plasma ceramide concentration increased significantly by 49% ($p<0.001$) in the SAT group. In contrast, there were no changes in plasma ceramides in the UNSAT or CARB groups. The increase in total plasma ceramides was significantly higher in the SAT as compared to the UNSAT ($p<0.05$) and the CARB ($p<0.001$) groups. This difference was independent of changes in body weight as determined by the significantly different intercepts of the linear regression lines between change in total plasma ceramides and change in body weight in the SAT vs. the UNSAT ($p<0.05$) and in the SAT vs. the CARB ($p<0.001$) groups.

The increase in total plasma ceramide concentration in the SAT group was due to increases in several long-chain ceramides (**Figure 3, Table S3**). Plasma concentrations of dihydroceramides (i.e. the precursors of ceramides in the *de novo* ceramide synthetic pathway, the species with

18:0 sphingoid base) were also increased in the SAT but not the other groups (**Figure 3, Table S3**).

Gut microbiota and LBP/sCD14

Serum LBP/sCD14, a marker of endotoxemia (16), increased significantly (4.3±1.0 vs. 4.7±1.1 (p<0.01)) in the SAT group but not in the other groups. The increase in LBP/sCD14 was significantly higher in the SAT as compared to UNSAT (p<0.05) and CARB (p<0.001) groups. Regarding gut microbiota, most (79%) of between-sample microbiota variation was explained by the subject (p<0.001, **Figure S4**), highlighting overall resilience of the individual-specific microbiota during overfeeding. We next analyzed individual taxa that were affected by overfeeding (**Figure S5**). The abundance of gram-negative Proteobacteria increased 3.6-fold during the SAT (p=0.038) but not the other diets (**Figure S6**). Other bacterial families remained unchanged.

Plasma lipids, adiponectin and liver enzymes

Baseline concentrations are shown in **Table 1**. Plasma HDL cholesterol increased significantly by 17% in the SAT (+0.3±0.3 mmol/l, p<0.01 for after vs. before) but not in the UNSAT (+0.1±0.3 mmol/l) or CARB (-0.1±0.2 mmol/l) groups. The increase in HDL cholesterol was significantly greater in the SAT than the CARB group (p<0.001). Plasma LDL cholesterol increased by 10% in the SAT group (+0.3±0.4 mmol/l, p<0.01) but remained unchanged in the UNSAT and CARB groups. There were no significant changes in plasma triglycerides or adiponectin in the groups. Plasma ALT increased significantly in the SAT (28±15 vs. 35±18 IU/L, p<0.05) but not in the UNSAT (26±9 vs. 27±5 IU/L) or CARB (24±11 vs. 28±18 IU/L) groups. Plasma AST increased in the SAT (26±5 vs. 29±6 IU/L, p<0.05) but remained unchanged in the UNSAT and CARB groups.

DISCUSSION

NAFLD has been shown to predict type 2 diabetes and cardiovascular disease in multiple studies even independent of obesity (1). It also increases the risk of progressive liver disease (17). It is therefore interesting to compare effects of different diets on liver fat content and understand the underlying mechanisms. We examined whether provision of excess calories as saturated (SAT) or unsaturated (UNSAT) fats or simple sugars (CARB) influences the metabolic response to overfeeding in overweight subjects. All overfeeding diets increased IHTG. The SAT diet induced a greater increase in IHTG than the UNSAT diet. The composition of the diet altered sources of excess IHTG. The SAT diet increased lipolysis, while the CARB diet stimulated DNL. The SAT but not the other diets increased multiple plasma ceramides, which increase the risk of cardiovascular disease independent of LDL cholesterol (18).

Compliance. The FA composition of liver TG is similar to that in VLDL (4). We monitored compliance by analyzing changes in FA composition of VLDL-TG. The SAT diet increased SFA while the UNSAT diet increased polyunsaturated FA (**Figure 1B**). The CARB diet also increased SFA, which are exclusive products of DNL (5). These data demonstrate that subjects were compliant, and are novel in showing that different diets have distinct effects on hepatic FA composition as determined from that in VLDL-TG. Weight gain averaged 1.2 kg in all subjects overeating 1000 kcal for 3 weeks. This weight gain is consistent with that (1.6 kg) observed by Riserus et al. in healthy subjects overeating 600 kcal/day for 7 weeks (2) but less than that observed by Harris et al. (2.3 kg) during the first 3 weeks of overfeeding 1000 kcal/day (19). As in the present study, inter-individual variation in the latter study was large and ranged from 1 to 7 kg after 8 weeks (19). We also observed slightly but not significantly less weight gain in subjects fed the UNSAT compared to the other diets. However, importantly the key findings, i.e. the greater increase in liver fat, lipolysis and ceramides by the SAT as compared to the UNSAT diet were independent of changes in body weight.

IHTG. Overfeeding increases IHTG (2,5,20). The SAT diet increased IHTG significantly more than the UNSAT diet in the face of similar energy excess and independent of changes in body weight. This is consistent with a previous study showing a greater increase in IHTG after overfeeding saturated than polyunsaturated fat (2). Similarly, an isocaloric saturated fat-enriched diet increases IHTG compared to polyunsaturated fat (21). High saturated fat intakes characterize subjects with NAFLD (22-23). Thus, diet composition influences IHTG and that saturated fat induces greater accumulation of IHTG than unsaturated fat.

Pathways of IHTG. Regarding the mechanisms underlying increased IHTG during overfeeding, direct quantification of sources of FAs in IHTG using stable isotopes and liver biopsies in subjects with elevated IHTG have shown that the majority of IHTG are derived from adipose tissue lipolysis (59%) and DNL (26%) (4). We found SAT to increase and UNSAT to decrease adipose tissue lipolysis. Lipolysis was traced using deuterated glycerol, which is not re-esterified in adipose tissue due to a lack of glycerol kinase. This contrasts S-FFA which concentration reflects net effects of lipolysis and lipogenesis. Overfeeding decreased S-FFA, as reported previously (20). There are no studies measuring overfeeding effects on lipolysis in humans. In mice high-saturated fat feeding stimulates lipolysis *via* inflammatory mediators (6). In keeping with such data, we found upregulation of multiple inflammation-related pathways in adipose tissue transcriptome. Polyunsaturated fatty acids inhibit lipolysis *via* activation of G-protein coupled receptor 120, which mediates anti-inflammatory and insulin-sensitizing effects (24-25). The opposite effects of the SAT and UNSAT diets on lipolysis, the major contributor to IHTG, could explain why SAT increased IHTG to a greater extent than the UNSAT diet.

Overfeeding simple sugars stimulates DNL, which produces exclusively SFA in humans and occurs mainly in the liver (5). Consistent with these data, the CARB diet increased hepatic DNL

and SFAs in VLDL-TG (**Figures 1B and 2A**). The CARB diet also induced multiple pathways related to carbohydrate metabolism in the adipose tissue transcriptome (**Figure 2D**).

IR and its mediators. The SAT diet induced IR. This is consistent with several studies showing that isocaloric substitution of saturated for monounsaturated (26-27) or polyunsaturated fat (28), or carbohydrates (27) ameliorates IR. Recently, a large prospective study reported intake of foods rich in SFA such as butter and cheese to increase the risk of type 2 diabetes (29).

SAT but not the other diets increased multiple plasma ceramides. TGs themselves are inert and do not confer IR (7). In mice, ceramides are key mediators of saturated fat-induced IR (8-10,30-33) and the most upregulated lipid species in inflamed adipose tissue in human NAFLD (34). SFAs and ceramides originating from *de novo* ceramide synthesis co-segregate with IR in human NAFLD (7). Saturated palmitoyl-CoA is an obligate precursor for the *de novo* pathway (8,30). The SAT diet thus may have induced IR *via* stimulating the *de novo* ceramide synthetic pathway in the liver. The SAT but not the other diets also increased markers of endotoxemia and upregulated genes related to gram-negative bacterial infection in adipose tissue. These changes could have contributed to SAT-induced lipolysis and *de novo* ceramide synthesis since in mice endotoxin induces both adipose tissue inflammation (11) and ceramide-dependent IR (10).

Limitations of our study include small sample size although largest of its kind (35). Another limitation is that we did not assess physical activity objectively during the study. It might also have been helpful to include a control group being overfed their habitual diet.

In conclusion, overfeeding either saturated or unsaturated fat or simple sugars for 3 weeks increases IHTG but its magnitude and the associated metabolic changes depend on the diet. Saturated fat induced highest increase in IHTG by stimulating adipose tissue lipolysis, the major

pathway of IHTG. Moreover, saturated fat induced insulin resistance and increased circulating concentrations of ceramides. In contrast to saturated fat, overfeeding of unsaturated fat led to a smaller increase in IHTG, decreased lipolysis and no change in ceramides. Simple sugars increased IHTG by stimulating DNL. Consistent with current dietary recommendations (36-38), the present study shows that saturated fat is the most harmful dietary constituent regarding IHTG accumulation. Since NAFLD increases the risk of type 2 diabetes, avoidance of foods rich in saturated fats might also help in prevention of diabetes.

ACKNOWLEDGEMENTS

Figure Legends

Figure 1. (A) Design of the study, (B) overfeeding-induced changes in fatty acid (FA) composition of VLDL-TG in the groups, (C) intrahepatic triglyceride (IHTG) before and after overfeeding, and (D) changes in IHTG between the groups. The subjects were randomized into overfeeding either saturated fat (SAT), unsaturated fat (UNSAT), or simple sugars (CARB). All subjects underwent metabolic studies at baseline and after 3 weeks of overfeeding. At these visits, intrahepatic triglyceride content was determined by proton magnetic resonance spectroscopy (^{1}H-MRS), hepatic *de novo* lipogenesis from ^{2}H$_{2}$O enrichment in VLDL-TG palmitate, adipose tissue lipolysis by ^{2}H$_{5}$-glycerol in the basal state and during euglycemic hyperinsulinemia, plasma ceramides by UHPLC-MS, and endotoxemia by fecal 16S rRNA and serum LBP/sCD14 ELISA. In addition, adipose tissue transcriptome was determined by microarray. Black bars denote the SAT group, white bars the UNSAT, and hatched bars the CARB group. In (B), the x-axis shows the change in % FA in VLDL-TG after versus before overfeeding and the y-axis the specific fatty acids in VLDL-TG. Data are shown as mean ± SEM. * $p<0.05$, ** $p<0.01$, *** $p<0.001$ within groups. † = $p<0.05$ between groups. B = before, A = after.

Figure 2. Overfeeding-induced changes in (A) hepatic *de novo* lipogenesis, (B) basal glycerol rate of appearance (R$_{a}$), (C) glycerol R$_{a}$ during euglycemic hyperinsulinemia, and (D) adipose tissue transcriptome. Black bars denote the saturated fat (SAT), white bars the unsaturated fat (UNSAT), and hatched bars the simple sugar (CARB) group. The y-axes indicate the change of mean values after versus before overfeeding within groups. Data are reported as mean ± SEM or in medians (interquartile ranges), as appropriate. *$p<0.05$, ** $p<0.01$, *** $p<0.001$. † = $p<0.05$ between groups, † † = $p<0.01$ between groups. The bubble grid shows the reporter test statistics (proportional to size and color intensity) comparing post- relative to pre-overfeeding

gene expression. Only pathways significant in at least one diet are shown (<5% false discovery rate).

Figure 3. Overfeeding-induced changes in individual plasma ceramides in the groups. In the heatmaps, each square indicates the $\log_2$ of the ratio between mean concentrations after versus before for an individual ceramide. The color key denotes the relationship between the color of the heatmap and $\log_2$ of the ratio between the means with 0 indicating no change. The y-axis denotes the fatty acyl chain structure (number of carbon atoms:number of double bonds) and the x-axis the sphingoid base species. *$p<0.05$, ** $p<0.01$, *** $p<0.001$.

REFERENCES

1. Yki-Järvinen H. Non-alcoholic fatty liver disease as a cause and a consequence of metabolic syndrome. Lancet Diabetes Endocrinol. 2014;2(11):901-10.
2. Rosqvist F, Iggman D, Kullberg J, Cedernaes J, Johansson HE, Larsson A, Johansson L, Ahlström H, Arner P, Dahlman I, Risérus U. Overfeeding polyunsaturated and saturated fat causes distinct effects on liver and visceral fat accumulation in humans. Diabetes. 2014;63(7):2356-68.
3. Mozaffarian D, Hao T, Rimm EB, Willett WC, Hu FB. Changes in diet and lifestyle and long-term weight gain in women and men. N Engl J Med. 2011;364(25):2392-404.
4. Donnelly KL, Smith CI, Schwarzenberg SJ, Jessurun J, Boldt MD, Parks EJ. Sources of fatty acids stored in liver and secreted via lipoproteins in patients with nonalcoholic fatty liver disease. J Clin Invest. 2005;115(5):1343-51.
5. Sevastianova K, Santos A, Kotronen A, Hakkarainen A, Makkonen J, Silander K, Peltonen M, Romeo S, Lundbom J, Lundbom N, Olkkonen VM, Gylling H, Fielding BA, Rissanen A, Yki-Järvinen H. Effect of short-term carbohydrate overfeeding and long-term weight loss on liver fat in overweight humans. Am J Clin Nutr. 2012;96(4):727-34.
6. Wueest S, Item F, Lucchini FC, Challa TD, Müller W, Blüher M, Konrad D. Mesenteric Fat Lipolysis Mediates Obesity-Associated Hepatic Steatosis and Insulin Resistance. Diabetes. 2016;65(1):140-8.
7. Luukkonen PK, Zhou Y, Sädevirta S, Leivonen M, Arola J, Orešič M, Hyötyläinen T, Yki-Järvinen H. Hepatic ceramides dissociate steatosis and insulin resistance in patients with non-alcoholic fatty liver disease. J Hepatol. 2016;64(5):1167-1175.
8. Chavez JA, Summers SA. A ceramide-centric view of insulin resistance. Cell Metab. 2012;15(5):585-94.
9. Xie C, Jiang C, Shi J, Gao X, Sun D, Sun L, Wang T, Takahashi S, Anitha M, Krausz KW, Patterson AD, Gonzalez FJ. An Intestinal Farnesoid X Receptor-Ceramide Signaling Axis Modulates Hepatic Gluconeogenesis in Mice. Diabetes. 2017;66(3):613-626.
10. Holland WL, Bikman BT, Wang LP, Yuguang G, Sargent KM, Bulchand S, Knotts TA, Shui G, Clegg DJ, Wenk MR, Pagliassotti MJ, Scherer PE, Summers SA. Lipid-induced insulin resistance mediated by the proinflammatory receptor TLR4 requires saturated fatty acid-induced ceramide biosynthesis in mice. J Clin Invest. 2011;121(5):1858-70.
11. Cani PD, Amar J, Iglesias MA, Poggi M, Knauf C, Bastelica D, Neyrinck AM, Fava F, Tuohy KM, Chabo C, Waget A, Delmée E, Cousin B, Sulpice T, Chamontin B, Ferrières J, Tanti JF, Gibson GR, Casteilla L, Delzenne NM, Alessi MC, Burcelin R. Metabolic endotoxemia initiates obesity and insulin resistance. Diabetes. 2007;56(7):1761-72.
12. Caesar R, Tremaroli V, Kovatcheva-Datchary P, Cani PD, Bäckhed F. Crosstalk between Gut Microbiota and Dietary Lipids Aggravates WAT Inflammation through TLR Signaling. Cell Metab. 2015;22(4):658-68.
13. Hodson L, Skeaff CM, Fielding BA. Fatty acid composition of adipose tissue and blood in humans and its use as a biomarker of dietary intake. Prog Lipid Res. 2008;47(5):348-80.
14. Yki-Järvinen H, Puhakainen I, Saloranta C, Groop L, Taskinen MR. Demonstration of a novel feedback mechanism between FFA oxidation from intracellular and intravascular sources. Am J Physiol. 1991;260(5 Pt 1):E680-9.
15. Luukkonen PK, Zhou Y, Nidhina Haridas PA, Dwivedi OP, Hyötyläinen T, Ali A, Juuti A, Leivonen M, Tukiainen T, Ahonen L, Scott E, Palmer JM, Arola J, Orho-Melander M, Vikman P, Anstee QM, Olkkonen VM, Orešič M, Groop L, Yki-Järvinen H. Impaired hepatic lipid synthesis from polyunsaturated fatty acids in TM6SF2 E167K variant carriers with NAFLD. J Hepatol. 2017;67(1):128-136.
16. Laugerette F, Alligier M, Bastard JP, Drai J, Chanséaume E, Lambert-Porcheron S, Laville M, Morio B, Vidal H, Michalski MC. Overfeeding increases postprandial endotoxemia in men:

Inflammatory outcome may depend on LPS transporters LBP and sCD14. Mol Nutr Food Res. 2014;58(7):1513-8.

17. Dongiovanni P, Stender S, Pietrelli A, Mancina RM, Cespiati A, Petta S, Pelusi S, Pingitore P, Badiali S, Maggioni M, Mannisto V, Grimaudo S, Pipitone RM, Pihlajamaki J, Craxi A, Taube M, Carlsson LMS, Fargion S, Romeo S, Kozlitina J, Valenti L. Causal relationship of hepatic fat with liver damage and insulin resistance in nonalcoholic fatty liver. J Intern Med. 2018;283(4):356-370.

18. Summers SA. Could Ceramides Become the New Cholesterol? Cell Metab. 2018;27(2):276-280.

19. Harris AM, Jensen MD, Levine JA. Weekly changes in basal metabolic rate with eight weeks of overfeeding. Obesity (Silver Spring). 2006;14(4):690-5.

20. Sobrecases H, Lê KA, Bortolotti M, Schneiter P, Ith M, Kreis R, Boesch C, Tappy L. Effects of short-term overfeeding with fructose, fat and fructose plus fat on plasma and hepatic lipids in healthy men. Diabetes Metab. 2010;36(3):244-6.

21. Bjermo H, Iggman D, Kullberg J, Dahlman I, Johansson L, Persson L, Berglund J, Pulkki K, Basu S, Uusitupa M, Rudling M, Arner P, Cederholm T, Ahlström H, Risérus U. Effects of n-6 PUFAs compared with SFAs on liver fat, lipoproteins, and inflammation in abdominal obesity: a randomized controlled trial. Am J Clin Nutr. 2012;95(5):1003-12.

22. Tiikkainen M, Bergholm R, Vehkavaara S, Rissanen A, Häkkinen AM, Tamminen M, Teramo K, Yki-Järvinen H. Effects of identical weight loss on body composition and features of insulin resistance in obese women with high and low liver fat content. Diabetes. 2003;52(3):701-7.

23. Musso G, Gambino R, De Michieli F, Cassader M, Rizzetto M, Durazzo M, Fagà E, Silli B, Pagano G. Dietary habits and their relations to insulin resistance and postprandial lipemia in nonalcoholic steatohepatitis. Hepatology. 2003;37(4):909-16.

24. Oh DY, Talukdar S, Bae EJ, Imamura T, Morinaga H, Fan W, Li P, Lu WJ, Watkins SM, Olefsky JM. GPR120 is an omega-3 fatty acid receptor mediating potent anti-inflammatory and insulin-sensitizing effects. Cell. 2010;142(5):687-98.

25. Wang M, Zhang X, Ma LJ, Feng RB, Yan C, Su H, He C, Kang JX, Liu B, Wan JB. Omega-3 polyunsaturated fatty acids ameliorate ethanol-induced adipose hyperlipolysis: A mechanism for hepatoprotective effect against alcoholic liver disease. Biochim Biophys Acta. 2017;1863(12):3190-3201.

26. Vessby B, Uusitupa M, Hermansen K, Riccardi G, Rivellese AA, Tapsell LC, Nälsén C, Berglund L, Louheranta A, Rasmussen BM, Calvert GD, Maffetone A, Pedersen E, Gustafsson IB, Storlien LH; KANWU Study. Substituting dietary saturated for monounsaturated fat impairs insulin sensitivity in healthy men and women: The KANWU Study. Diabetologia. 2001;44(3):312-9.

27. Pérez-Jiménez F, López-Miranda J, Pinillos MD, Gómez P, Paz-Rojas E, Montilla P, Marín C, Velasco MJ, Blanco-Molina A, Jiménez Pereпérez JA, Ordovás JM. A Mediterranean and a high-carbohydrate diet improve glucose metabolism in healthy young persons. Diabetologia. 2001;44(11):2038-43.

28. Summers LK, Fielding BA, Bradshaw HA, Ilic V, Beysen C, Clark ML, Moore NR, Frayn KN. Substituting dietary saturated fat with polyunsaturated fat changes abdominal fat distribution and improves insulin sensitivity. Diabetologia. 2002;45(3):369-77.

29. Guasch-Ferré M, Becerra-Tomás N, Ruiz-Canela M, Corella D, Schröder H, Estruch R, Ros E, Arós F, Gómez-Gracia E, Fiol M, Serra-Majem L, Lapetra J, Basora J, Martín-Calvo N, Portoles O, Fitó M, Hu FB, Forga L, Salas-Salvadó J. Total and subtypes of dietary fat intake and risk of type 2 diabetes mellitus in the Prevención con Dieta Mediterránea (PREDIMED) study. Am J Clin Nutr. 2017;105(3):723-735.
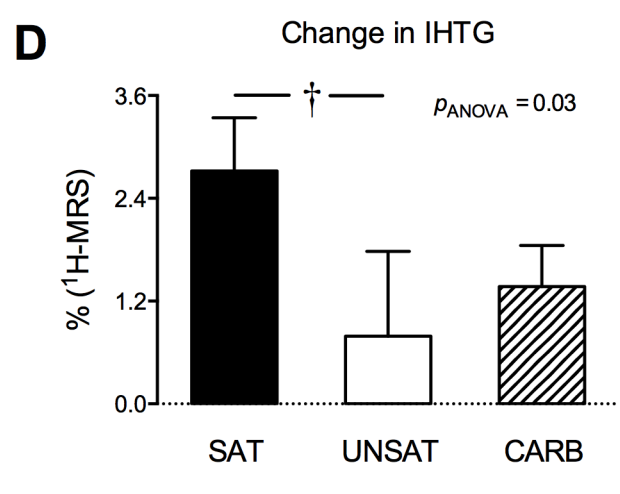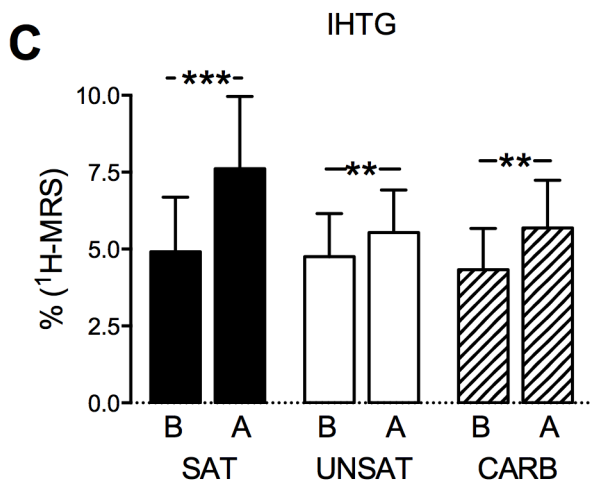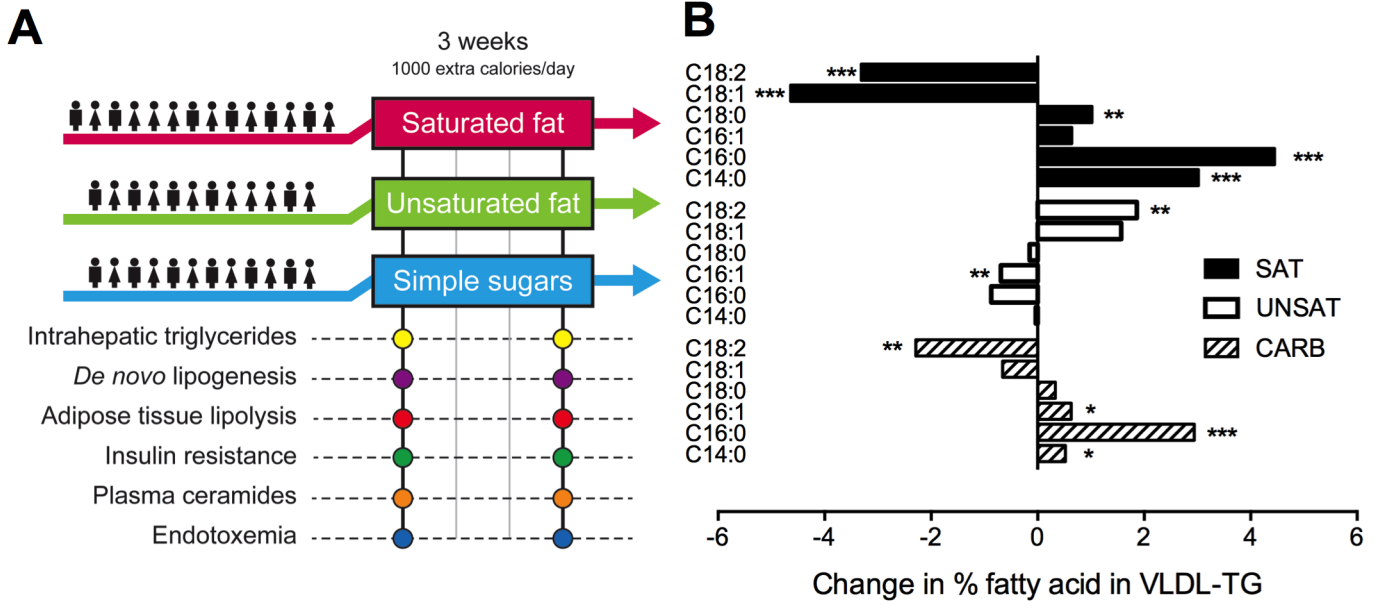
30. Holland WL, Brozinick JT, Wang LP, Hawkins ED, Sargent KM, Liu Y, Narra K, Hoehn KL, Knotts TA, Siesky A, Nelson DH, Karathanasis SK, Fontenot GK, Birnbaum MJ, Summers

SA. Inhibition of ceramide synthesis ameliorates glucocorticoid-, saturated-fat-, and obesity-induced insulin resistance. Cell Metab. 2007;5(3):167-79.

31. Raichur S, Wang ST, Chan PW, Li Y, Ching J, Chaurasia B, Dogra S, Öhman MK, Takeda K, Sugii S, Pewzner-Jung Y, Futerman AH, Summers SA. CerS2 haploinsufficiency inhibits β-oxidation and confers susceptibility to diet-induced steatohepatitis and insulin resistance. Cell Metab. 2014;20(4):687-95.

32. Turpin SM, Nicholls HT, Willmes DM, Mourier A, Brodesser S, Wunderlich CM, Mauer J, Xu E, Hammerschmidt P, Brönneke HS, Trifunovic A, LoSasso G, Wunderlich FT, Kornfeld JW, Blüher M, Krönke M, Brüning JC. Obesity-induced CerS6-dependent C16:0 ceramide production promotes weight gain and glucose intolerance. Cell Metab. 2014;20(4):678-86.

33. Xia JY, Holland WL, Kusminski CM, Sun K, Sharma AX, Pearson MJ, Sifuentes AJ, McDonald JG, Gordillo R, Scherer PE. Targeted Induction of Ceramide Degradation Leads to Improved Systemic Metabolism and Reduced Hepatic Steatosis. Cell Metab. 2015;22(2):266-278.

34. Kolak M, Westerbacka J, Velagapudi VR, Wågsäter D, Yetukuri L, Makkonen J, Rissanen A, Häkkinen AM, Lindell M, Bergholm R, Hamsten A, Eriksson P, Fisher RM, Oresic M, Yki-Järvinen H. Adipose tissue inflammation and increased ceramide content characterize subjects with high liver fat content independent of obesity. Diabetes. 2007;56(8):1960-8.

35. Yki-Järvinen H. Nutritional Modulation of Non-Alcoholic Fatty Liver Disease and Insulin Resistance. Nutrients. 2015;7(11):9127-38.

36. US Department of Health and Human Services; US Department of Agriculture. 2015-2020 Dietary Guidelines for Americans. 8th ed. Washington, DC: US Dept of Health and Human Services; December 2015. http://www.health.gov/DietaryGuidelines. Accessed August 11, 2017.

37. American Diabetes Association. 4. Lifestyle Management: Standards of Medical Care in Diabetes-2018. Diabetes Care. 2018;41(Suppl 1):S38-S50. doi: 10.2337/dc18-S004.

38. Sacks FM, Lichtenstein AH, Wu JHY, Appel LJ, Creager MA, Kris-Etherton PM, Miller M, Rimm EB, Rudel LL, Robinson JG, Stone NJ, Van Horn LV; American Heart Association. Dietary Fats and Cardiovascular Disease: A Presidential Advisory From the American Heart Association. Circulation. 2017;136(3):e1-e23.

Table 1. Baseline clinical characteristics of the study subjects according to diet group.

	SAT	UNSAT	CARB
Group size (n)	14	12	12
Age (years)	48 ± 8	52 ± 10	45 ± 10
Gender (n, women/men)	8/6	7/5	6/6
BMI (kg/m^2)	30 ± 6	31 ± 6	33 ± 6
Fat free mass (kg)	58.6 ± 9.7	60.2 ± 13.3	61.9 ± 12.3
Liver fat (^{1}H-MRS, %)	4.9 ± 6.6	4.8 ± 4.9	4.3 ± 4.7
Visceral adipose tissue (MRI, cm^3)	1940 ± 1605	2019 ± 1328	2014 ± 1217
Subcutaneous adipose tissue (MRI, cm^3)	4770 ± 2152	4732 ± 2350	5133 ± 2154
Waist circumference (cm)	97 ± 17	98 ± 13	102 ± 12
Waist to hip ratio	0.90 ± 0.10	0.90 ± 0.07	0.92 ± 0.06
LBP/sCD14	4.3 ± 1.0	4.6 ± 0.9	4.9 ± 1.6
fP-Glucose (mmol/l)	5.6 ± 0.6	5.7 ± 0.6	5.9 ± 0.7
Impaired fasting glucose (>5.6 mmol/l)	8	6	8
fS-Insulin (mU/l)	8.1 (5.8 – 11.9)	9.1 (6.5 – 14.6)	10.3 (6.2 – 19.2)
HOMA-IR	1.9 (1.3 – 3.2)	2.3 (1.6 – 4.0)	2.8 (1.7 – 5.0)
Systolic BP (mmHg)	133 ± 15	134 ± 17	139 ± 20
Diastolic BP (mmHg)	80 ± 11	83 ± 7	85 ± 13
fP-Triglycerides (mmol/l)	1.1 ± 1.0	1.1 ± 0.4	1.4 ± 0.6
fP-HDL cholesterol (mmol/l)	1.62 ± 0.39	1.61 ± 0.47	1.53 ± 0.37
fP-LDL cholesterol (mmol/l)	3.2 ± 1.0	3.4 ± 0.8	3.5 ± 0.8
fS-FFA (µmol/l)	556 ± 217	610 ± 181	639 ± 225
fP-Adiponectin (µg/ml)	11.0 ± 4.3	10.5 ± 5.7	10.3 ± 5.8
fP-ALT (IU/l)	28 ± 15	26 ± 9	24 ± 11
fP-AST (IU/l)	26 ± 5	27 ± 7	26 ± 6
PNPLA3 (CC/CG/GG) (n)	9/5/0	7/4/1	5/4/2

Data are in n (%), means ± SD or median (25th-75th percentile), as appropriate. There were no significant differences in any variable between the groups using ANOVA, Kruskal-Wallis and Fisher's exact test, as appropriate.

A

3 weeks
1000 extra calories/day

Saturated fat

Unsaturated fat

Simple sugars

Intrahepatic triglycerides
De novo lipogenesis
Adipose tissue lipolysis
Insulin resistance
Plasma ceramides
Endotoxemia

B

C18:2 ***
C18:1 ***
C18:0 **
C16:1
C16:0 ***
C14:0 ***
C18:2 **
C18:1
C18:0
C16:1 **
C16:0
C14:0
C18:2 **
C18:1
C18:0
C16:1 *
C16:0 ***
C14:0 *

SAT
UNSAT
CARB

-6   -4   -2   0   2   4   6

Change in % fatty acid in VLDL-TG

C

IHTG

% (^{1}H-MRS)

10.0
7.5
5.0
2.5
0.0

- *** -
** -
-- ** -

B   A   B   A   B   A
SAT   UNSAT   CARB

D

Change in IHTG

% (^{1}H-MRS)

3.6
2.4
1.2
0.0

-- † --
$p_{ANOVA} = 0.03$

SAT   UNSAT   CARB

A Change in *de novo* lipogenesis

p_{ANOVA}=0.49

μmol/L

310 · 190 · 70 · -50

SAT · UNSAT · CARB

*
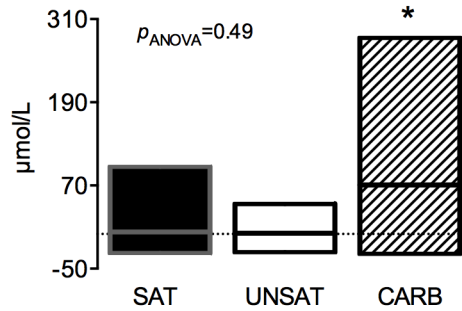
B Change in basal glycerol R_a

μmol/kg·min

1.2 · 0.6 · 0.0 · -0.6

p_{ANOVA}=0.22

SAT · UNSAT · CARB
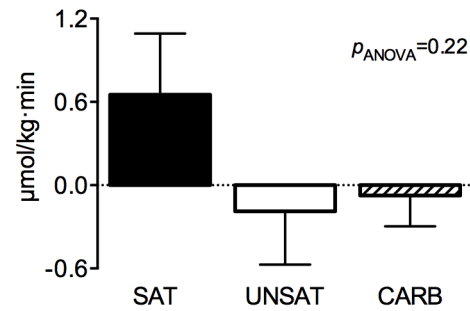
C Change in glycerol R_a during euglycemic hyperinsulinemia

μmol/kg·min

0.4 · 0.1 · -0.2 · -0.5

p_{ANOVA}=0.004

*

*

†† · †

SAT · UNSAT · CARB

D

SAT UNSAT CARB

PATHOGENIC ESCHERICHIA COLI INFECTION
NATURAL KILLER CELL MEDIATED CYTOTOXICITY
NOD LIKE RECEPTOR SIGNALING PATHWAY
LEUKOCYTE TRANSENDOTHELIAL MIGRATION
GLYCEROLIPID METABOLISM
PROPANOATE METABOLISM
ADHERENS JUNCTION
GLYOXYLATE AND DICARBOXYLATE METABOLISM
PPAR SIGNALING PATHWAY
CITRATE CYCLE TCA CYCLE
BIOSYNTHESIS OF UNSATURATED FATTY ACIDS
OXIDATIVE PHOSPHORYLATION
ECM RECEPTOR INTERACTION
INTESTINAL IMMUNE NETWORK FOR IGA PRODUCTION
HEMATOPOIETIC CELL LINEAGE
CHEMOKINE SIGNALING PATHWAY
PYRUVATE METABOLISM
ANTIGEN PROCESSING AND PRESENTATION
FRUCTOSE AND MANNOSE METABOLISM
PENTOSE PHOSPHATE PATHWAY
GLYCOLYSIS GLUCONEOGENESIS
VALINE LEUCINE AND ISOLEUCINE BIOSYNTHESIS
PRIMARY IMMUNODEFICIENCY
PRIMARY BILE ACID BIOSYNTHESIS
CELL ADHESION MOLECULES CAMS
CYTOKINE CYTOKINE RECEPTOR INTERACTION
RIBOSOME
LYSOSOME

-6 -3 0 3 6

Supplementary Material for: Saturated Fat is More Metabolically Harmful for the Human Liver than Unsaturated Fat or Simple Sugars

Panu K. Luukkonen[1,2], Sanja Sädevirta[1,2], You Zhou[1,3], Brandon Kayser[4], Ashfaq Ali[5], Linda Ahonen[5], Susanna Lallukka[1,2], Véronique Pelloux[4], Melania Gaggini[6], Ching Jian[7], Antti Hakkarainen[8], Nina Lundbom[8], Helena Gylling[2], Anne Salonen[7], Matej Orešič[5,9,10], Tuulia Hyötyläinen[5,11], Marju Orho-Melander[12], Aila Rissanen[13], Amalia Gastaldelli[6], Karine Clément[4,14], Leanne Hodson[15], Hannele Yki-Järvinen[1,2,16]

[1]Minerva Foundation Institute for Medical Research, Helsinki, Finland; [2]Department of Medicine, University of Helsinki and Helsinki University Central Hospital, Helsinki, Finland; [3]Systems Immunity University Research Institute and Division of Infection and Immunity, School of Medicine, Cardiff University, Cardiff, United Kingdom; [4]Sorbonne Universités, INSERM, UMRS 1166, Nutriomics team, ICAN, F-75013, Paris, France; [5]Steno Diabetes Center, Gentofte, Denmark; [6]Institute of Clinical Physiology, CNR, Pisa, Italy; [7]Immunobiology Research Program, Department of Bacteriology and Immunology, University of Helsinki; [8]Helsinki Medical Imaging Centre, Radiology, Helsinki University Hospital and University of Helsinki; [9]School of Medical Sciences, Örebro University, Örebro, Sweden; [10]Turku Centre for Biotechnology, University of Turku and Åbo Akademi University, Turku, Finland; [11]Department of Chemistry, Örebro University, Örebro, Sweden; [12]Lund University, Malmö, Sweden; [13]Obesity Research Unit, Department of Psychiatry, Helsinki University Central Hospital; [14]Assistance Publique-Hôpitaux de Paris (AP-HP), Pitié-Salpêtrière Hospital, Nutrition Department F-75013, Paris, France; [15]Oxford Centre for Diabetes, Endocrinology and Metabolism, University of Oxford, Oxford, UK; [16]Corresponding Author

Table of contents

Adipose tissue transcriptome

In the beginning of the study, after indirect calorimetry, a needle aspiration biopsy from abdominal subcutaneous adipose tissue was obtained under 1% lidocaine anesthesia and immediately frozen in liquid nitrogen and stored at −80°C until analysis. Total RNA was isolated using the RNeasy Lipid Tissue Mini Kit (Qiagen, Valencia, CA).

Bioinformatics. The Illumina HumanHT12v4 microarray chips (Illumina, San Diego, CA) were annotated using the IlluminaHumanv4.db from Bioconductor. A standard non-specific filtering approach was used to extract genes most likely to be expressed in the tissue and to ultimately limit the number of tests to genes of interest. Specifically, probes without annotation to a gene were removed, and if multiple probes matched to a gene, only the probe with the highest interquartile range across samples was included. Finally, only genes with inter-quartile range greater than the median of all genes were included. KEGG pathways were downloaded from the Molecular Signatures Database (http://software.broadinstitute.org/gsea/msigdb/collections.jsp#C2). To limit the number of tests to pathways of interest, unrelated pathways were removed e.g. Huntington's disease.

Statistical analysis. The pre/post comparisons within each diet were computed using LIMMA (1). Specifically, the two factors (time and diet) were converted into a single factor with 6 levels, and after running the full model, contrast tests between levels of interest were performed (e.g. Diet 1-Pre vs Diet 1-Post). The model was analyzed as a multi-level model to account for repeated measures. Array-quality weights were estimated and included in the model. Details of the LIMMA procedure can be found in the comprehensive manual (2).

For the reporter features analysis (3), log2 fold-change and unadjusted p-values from the LIMMA analysis were used as input. Statistical significance was determined from the null distribution and gene sets were limited to those with more than 3 genes and no more than 200. Otherwise, default parameters were used. Distinctly up- and down-regulated pathways were used to determine pathway enrichment in the specific direction. P-values were adjusted to the Benjamini-Hochberg false discovery rate.

Gut microbiota

Bacterial DNA was extracted from fecal samples using mechanical cell lysis that efficiently extracts bacterial community DNA as previously described (4). Illumina MiSeq paired-end sequencing of the hypervariable V3-V4 regions of the 16S rRNA gene was performed according to the manual from Illumina except that the libraries were prepared with single-step PCR, i.e. by amplifying the 16S rRNA gene fragment together with barcoded primers, the latter adapted from Kozich et al (5). The multiplex PCR reaction is comprised of 1 ng/ul template, 1X Phusion® Master Mix (ThermoFisher, F-531L), 0.25 uM V3-V4 locus specific primers and 0.375 uM dual-index barcodes. The PCR was run under the following settings: 98 °C for 30 s, 27 cycles of 98 °C for 10 s, 62 °C for 30 s, 72 °C for 15 s and finally 10 min at 72 °C, where after the samples were stored at 4 °C. The size of the PCR product was expected to be ~640 base pairs (bp) and verified on a Bioanalyzer DNA 1000 chip (Agilent Technology, Santa Clara, CA, USA). The PCR clean-up was performed with AMPure XP beads (Beckman Coulter, Copenhagen, Denmark) and confirmation of the right size of the target was performed on a Bioanalyzer DNA 1000 chip (Agilent Technology, CA, USA). The pooled libraries were sequenced at the sequencing unit of the Institute for Molecular Medicine Finland (FIMM), Helsinki, Finland with an Illumina MiSeq instrument using paired end 2 × 300 bp reads and a MiSeq v3 reagent kit with 5% PhiX as spike-in.

Sequencing data preprocessing, analysis and statistics

The forward reads were truncated to length of 150 bases with mare's "ProcessReads" command. We used default settings for minimum quality score and maximum expected errors. Reads with prevalence below 0.01% were removed. Chimera removal and dereplication of the reads was done using USEARCH8 (6). Truncated, filtered and dereplicated reads were annotated using the Silva database (7). The median read count per sample after preprocessing was 68797 (range 296 −148 604). The data analysis was done without rarefaction or transformations utilizing statistical and visualization tools included in the mare-package (8). The number of reads was used as an offset in all statistical models. Community dissimilarity was estimated with principal coordinates analysis (PCoA) using Bray-Curtis dissimilarity as the distance measure. PCoA was calculated with capscale function of R package vegan and Bray-Curtis dissimilarities with function vegdist of the same package (9). Permutational multivariate analysis of variance using distance matrices was performed with adonis function in package vegan to calculate the relative contribution of different factors in the microbiota

variation. Taxonomic richness was estimated as the number of observed OTUs after clustering the reads to operational taxonomic units (OTUs) using USEARCH8. Comparison of the abundance of bacterial genera between two time points in each intervention group was performed using generalized linear mixed models within "GroupTest" function of the mare package using subject as the random factor. This function uses the glmmADMB package (generalized linear mixed models built on AD Model Builder) of R software on background and assumes negative binomial distribution of abundance.

DNL methodology

Fasting DNL was assessed based on the incorporation of deuterium from ^2H_2O in plasma water (Finnigan GasBench-II, ThermoFisher Scientific, UK) into VLDL-TG palmitate using gas chromatography/mass spectrometry (GC/MS) with monitoring ions with mass-to-charge ratios (*m/z*) of 270 (M+0) and 271 (M+1) (10).

For the calculation of DNL in VLDL-TG using the mass isotopomer distributions, the maximum number of deuterium molecules synthesized from plasma palmitate was assumed to be 22 (11). When constant enrichment in the precursor pool (plasma water) was obtained, F was the enrichment of palmitate synthesized during the time between the loading dose of ^2H_2O and the collection time. When isotopic equilibrium in the product pool (palmitate) was obtained, F was constant. F = plasma palmitate enrichment/(22 × plasma deuterium enrichment). The percentage of *de novo* lipogenesis (%DNL) was calculated by multiplying F by 100%. Absolute DNL was calculated by multiplying %DNL and the concentration of TG in VLDL (12).

Consistently with a number of previous studies (10, 12-18), we used deuterated water with less than 24 hour loading for measurements of DNL. If the labelling period was longer, it is likely that we would have found higher rates of DNL. However, then it would have been also more challenging to account for differences in the recirculation of labeled fatty acids. A limitation of measuring DNL after an overnight fast only, is that we were unable to assess the synthesis of other fatty acids from DNL such as C16:1n-7 and C18:0 as done by Wilke et al. (Diabetologia 2009) as the labeling period (~12 h) was not long enough.

Although we have anecdotal evidence that 3 weeks is long enough to clear the majority of labeled lipid products from the first study on the day before each of the metabolic study days,

a blood sample was taken for measurement of background enrichment of ^{2}H in plasma water and VLDL-TG palmitate for measurement of DNL. Therefore we were able to account for any differences in plasma water and VLDL-TG for the second visit. Regarding other labeled precursors that may have been generated from the ^{2}H$_2$O administered at baseline, we did not measure labeling of ^{2}H-FFA palmitate in this study, as we have in previous studies found it to be minimal.

FA composition of VLDL-TG

VLDL was isolated by ultracentrifugation as described (19). Total lipids were extracted (20) and FA methyl esters (FAMEs) prepared from TG as described (21). Separation and quantification (expressed as mol%) of FAMEs was achieved on a HP6890 GC (Agilent Technologies, Stockport, UK) with flame ionisation detection.

REFERENCES

1. Smyth GK: Linear models and empirical bayes methods for assessing differential expression in microarray experiments. Stat Appl Genet Mol Biol 2004

2. Smyth GK, Ritchie M, Thorne N, Wettenhall J, Shi… W: Limma: Linear Models for Microarray and RNA-Seq Data User's Guide. Citeseer 2002

3. Väremo L, Nielsen J, Nookaew I: Enriching the gene set analysis of genome-wide data by incorporating directionality of gene expression and combining statistical hypotheses and methods. Nucleic Acids Res 41:4378-4391, 2013

4. Salonen A, Nikkila J, Jalanka-Tuovinen J, Immonen O, Rajilic-Stojanovic M, Kekkonen RA, et al. (2010). Comparative analysis of fecal DNA extraction methods with phylogenetic microarray: effective recovery of bacterial and archaeal DNA using mechanical cell lysis. J Microbiol Methods. 81(2):127-34.

5. Kozich JJ, Westcott SL, Baxter NT, Highlander SK, Schloss PD. (2013). Development of a dual-index sequencing strategy and curation pipeline for analyzing amplicon sequence data on the MiSeq Illumina sequencing platform. Appl Environ Microbiol. 79(17):5112-20.

6. Edgar RC. (2010). Search and clustering orders of magnitude faster than BLAST. Bioinformatics. 26(19):2460-1.

7. Quast C, Pruesse E, Yilmaz P, Gerken J, Schweer T, Yarza P, et al. (2012). The SILVA ribosomal RNA gene database project: improved data processing and web-based tools. Nucleic Acids Res. gks1219.

8. Korpela K. (2016). mare: Microbiota Analysis in R Easily. R package version 10" 23-Apr-2016.

9. Oksanen JFGB, R. Kindt, P. Legendre, P.R. Minchin, R.B. O'Hara, G.L. Simpson, P. Solymos, M.H.H. Stevens, H.Wagner. (2011). Package 'vegan' version 2.0-2.

10. Semple RK, Sleigh A, Murgatroyd PR, et al. (2009). Postreceptor insulin resistance contributes to human dyslipidemia and hepatic steatosis. J Clin Invest. 119(2):315-22.

11. Diraison F, Pachiaudi C, Beylot M. Measuring lipogenesis and cholesterol synthesis in humans with deuterated water: use of simple gas chromatographic/mass spectrometric techniques. J Mass Spectrom. 1997;32(1):81-6.

12. Santoro N, Caprio S, Pierpont B, et al. (2015). Hepatic De Novo Lipogenesis in Obese Youth Is Modulated by a Common Variant in the GCKR Gene. J Clin Endocrinol Metab. 100(8):E1125-32.

13. Matikainen N, Adiels M, Söderlund S, Stennabb S, Ahola T, Hakkarainen A, Borén J, Taskinen MR. Hepatic lipogenesis and a marker of hepatic lipid oxidation, predict postprandial responses of triglyceride-rich lipoproteins. Obesity (Silver Spring). 2014;22(8):1854-9.

14. Lambert JE, Ramos-Roman MA, Browning JD, Parks EJ. Increased de novo lipogenesis is a distinct characteristic of individuals with nonalcoholic fatty liver disease. Gastroenterology. 2014;146(3):726-35.

15. Pramfalk C, Pavlides M, Banerjee R, McNeil CA, Neubauer S, Karpe F, Hodson L. Sex-Specific Differences in Hepatic Fat Oxidation and Synthesis May Explain the Higher Propensity for NAFLD in Men. J Clin Endocrinol Metab. 2015;100(12):4425-33.

16. Pramfalk C, Pavlides M, Banerjee R, McNeil CA, Neubauer S, Karpe F, Hodson L. Fasting Plasma Insulin Concentrations Are Associated With Changes in Hepatic Fatty Acid Synthesis and Partitioning Prior to Changes in Liver Fat Content in Healthy Adults. Diabetes. 2016;65(7):1858-67.

17. Hodson L, Banerjee R, Rial B, Arlt W, Adiels M, Boren J, Marinou K, Fisher C, Mostad IL, Stratton IM, Barrett PH, Chan DC, Watts GF, Harnden K, Karpe F, Fielding BA.

Menopausal Status and Abdominal Obesity Are Significant Determinants of Hepatic Lipid Metabolism in Women. J Am Heart Assoc. 2015;4(10):e002258.

18. Hazlehurst JM, Oprescu AI, Nikolaou N, Di Guida R, Grinbergs AE, Davies NP, Flintham RB, Armstrong MJ, Taylor AE, Hughes BA, Yu J, Hodson L, Dunn WB, Tomlinson JW. Dual-5α-Reductase Inhibition Promotes Hepatic Lipid Accumulation in Man. J Clin Endocrinol Metab. 2016;101(1):103-13.

19. Sevastianova K, Santos A, Kotronen A, Hakkarainen A, Makkonen J, Silander K, Peltonen M, Romeo S, Lundbom J, Lundbom N, Olkkonen VM, Gylling H, Fielding BA, Rissanen A, Yki-Järvinen H. Effect of short-term carbohydrate overfeeding and long-term weight loss on liver fat in overweight humans. Am J Clin Nutr. 2012;96(4):727-34.

20. Folch J, Lees M, Sloane Stanley GH. (1957). A simple method for the isolation and purification of total lipides from animal tissues. J Biol Chem. 226(1): 497-509.

21. Heath RB, Karpe F, Milne RW, et al. (2003). Selective partitioning of dietary fatty acids into the VLDL TG pool in the early postprandial period. J Lipid Res. 44(11):2065-72.
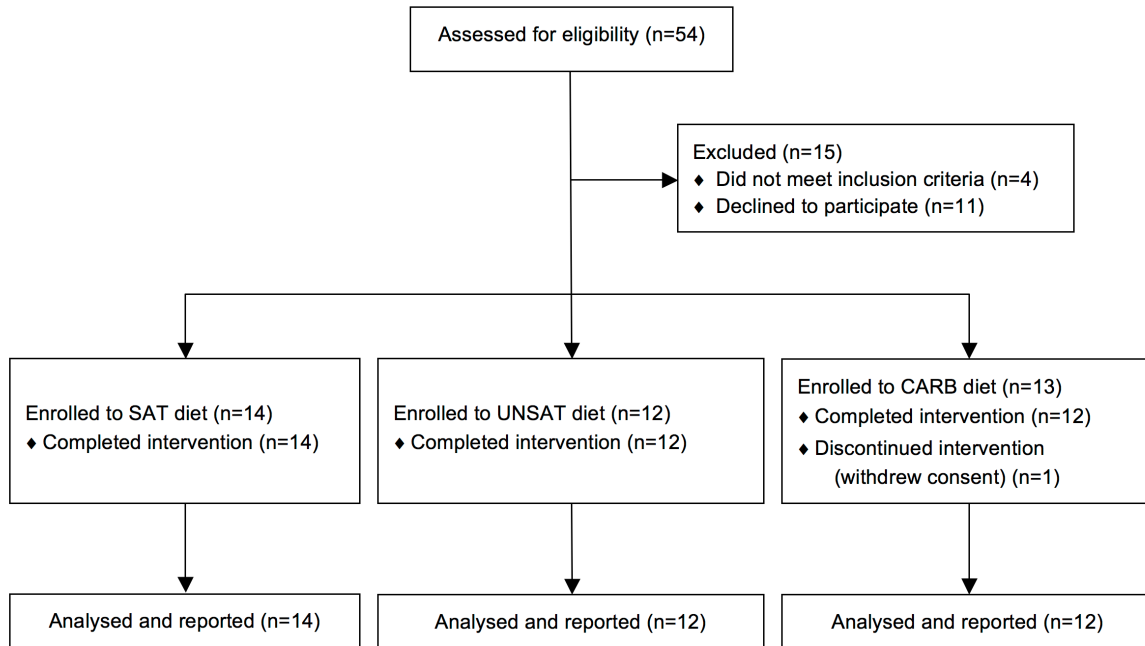
Supplementary Figures

Figure S1. Study flow chart. A total of 54 subjects were assessed for eligibility, 39 of whom were considered eligible. One subject withdrew from the study. Data were collected and analyzed on 14 subjects enrolled to the SAT diet, 12 subjects enrolled to the UNSAT diet, and 12 subjects enrolled to the CARB diet.
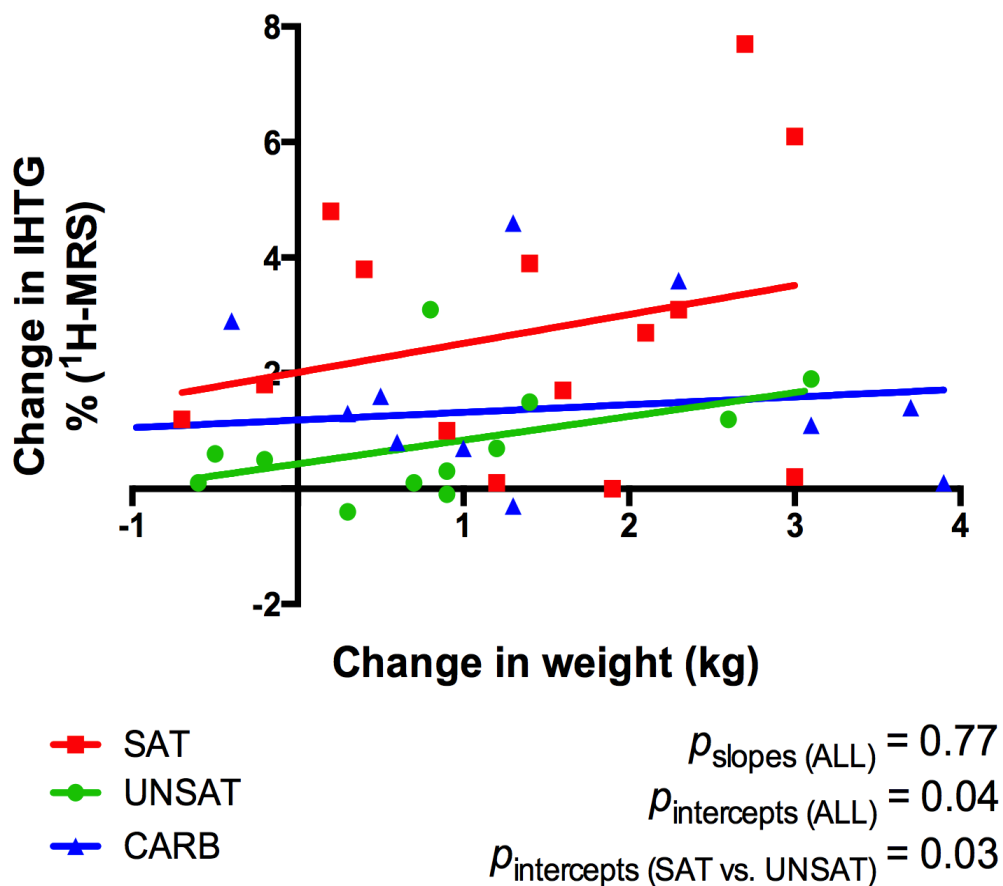
$p_{\text{slopes (ALL)}} = 0.77$

$p_{\text{intercepts (ALL)}} = 0.04$

$p_{\text{intercepts (SAT vs. UNSAT)}} = 0.03$

Figure S2. Linear regression between change in intrahepatic triglycerides (IHTG) and change in weight in the diet groups. The y-axis denotes the change in IHTG after versus before overfeeding as %-units determined by proton magnetic resonance spectroscopy (^{1}H-MRS). The x-axis denotes the change in body weight in kilograms after versus before overfeeding. Red symbols and line = saturated fat (SAT) group; green symbols and line = unsaturated fat (UNSAT) group; blue symbols and line = simple sugar (CARB) group.
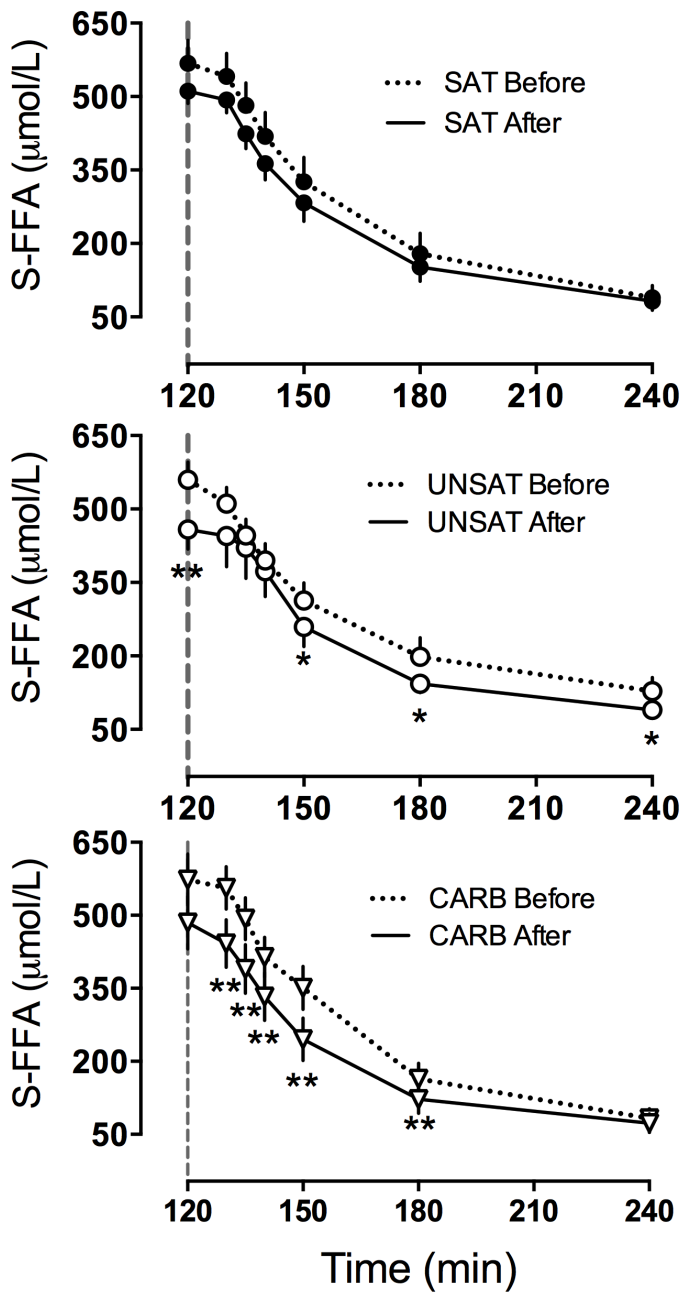
Figure S3. Serum free fatty acid (FFA) concentrations during euglycemic hyperinsulinemic clamp before and after the overfeeding. SAT = saturated fat (panel on the top), UNSAT = unsaturated fat (panel in the middle), CARB = simple sugar group (panel on the bottom). The x-axes denote serum FFA concentration and the y-axes time from the beginning of the study (euglycemic hyperinsulinemic clamp was started at 120 minutes). *p<0.05, **p<0.01.
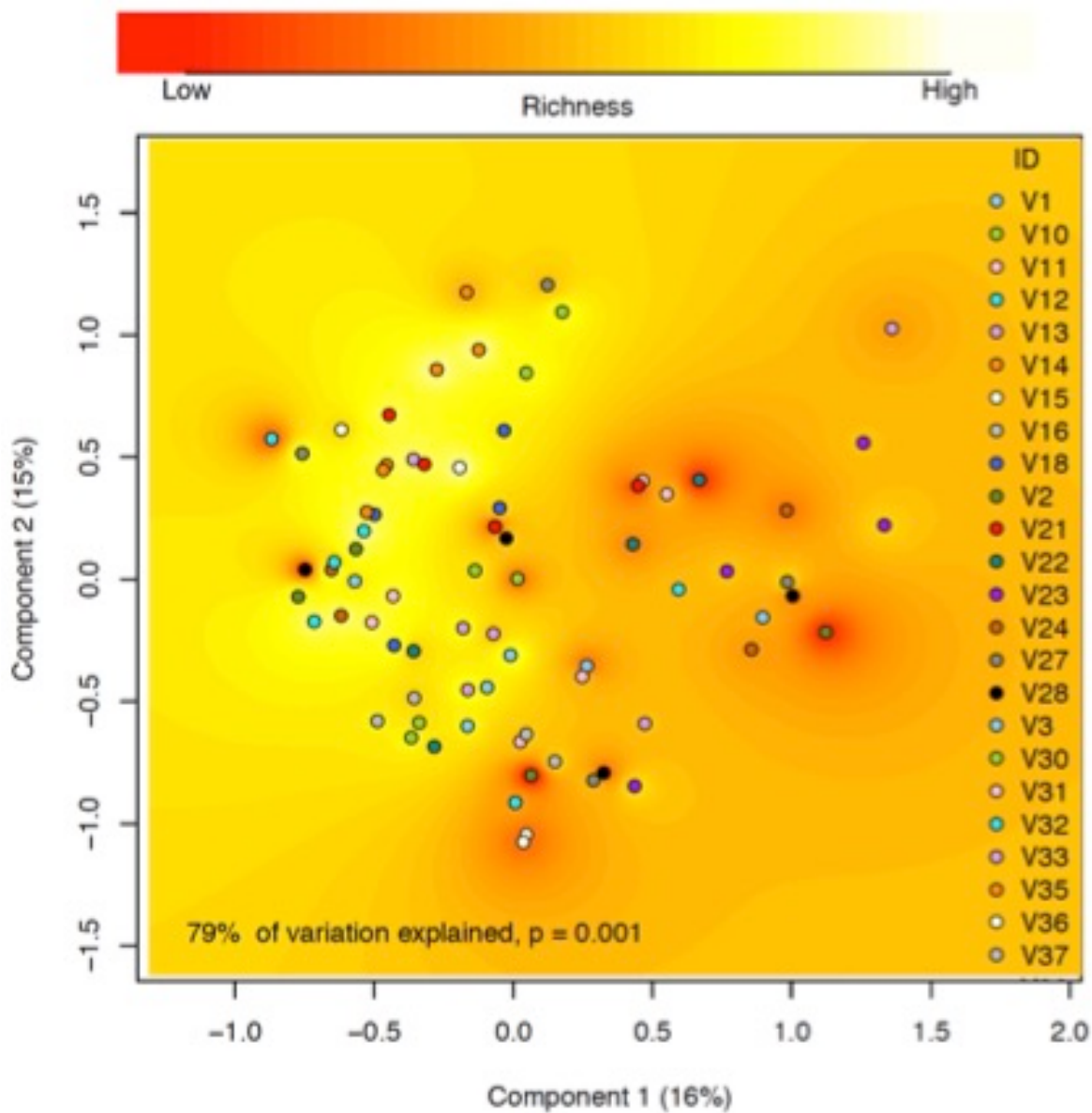
Figure S4. Principal coordinates analysis (PCoA) plot based on Bray-Curtis dissimilarity of all the microbiota samples, coloured according to the subject. The background colour indicates microbiota richness. Permutational multivariate analysis of variance was used to calculate the explanatory power of the subject.
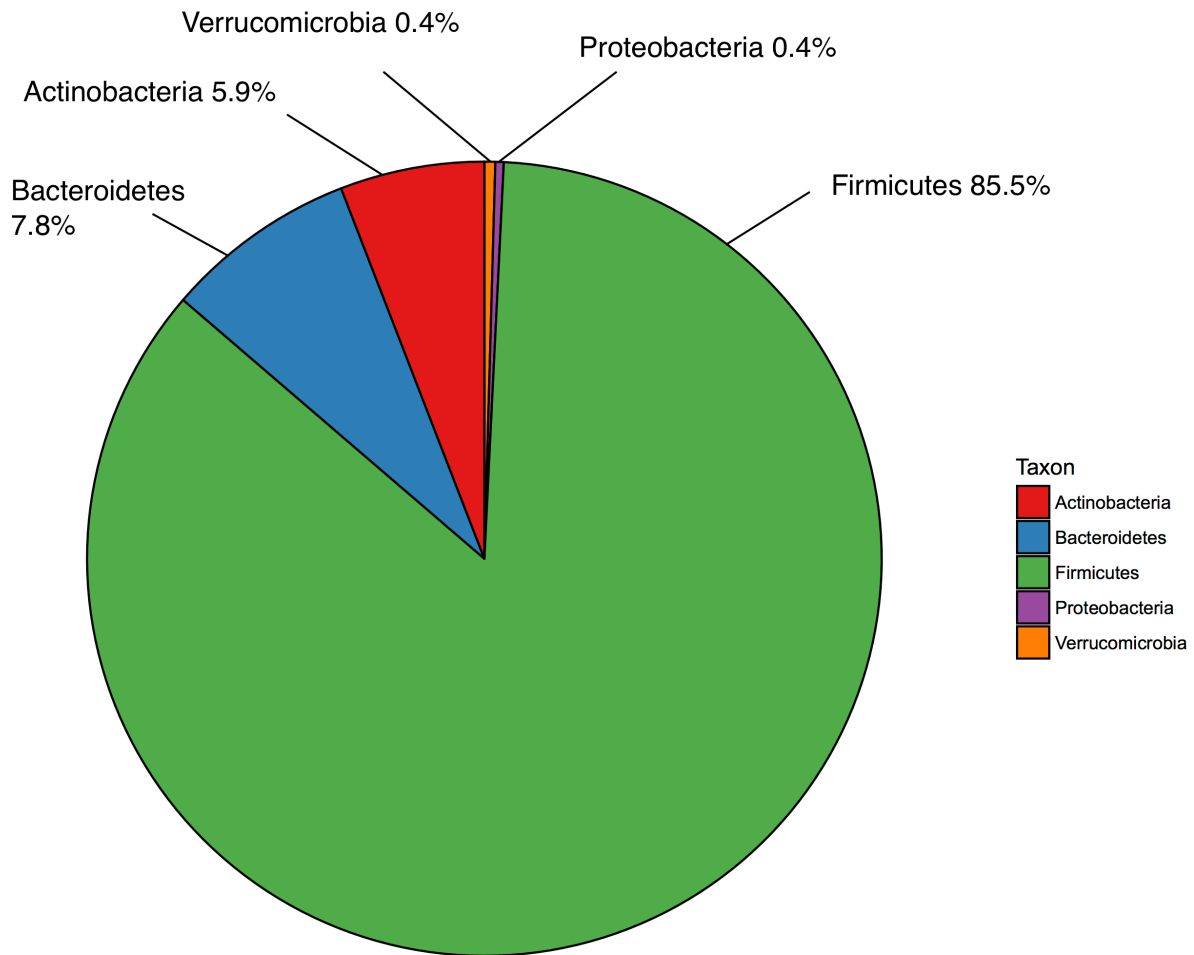
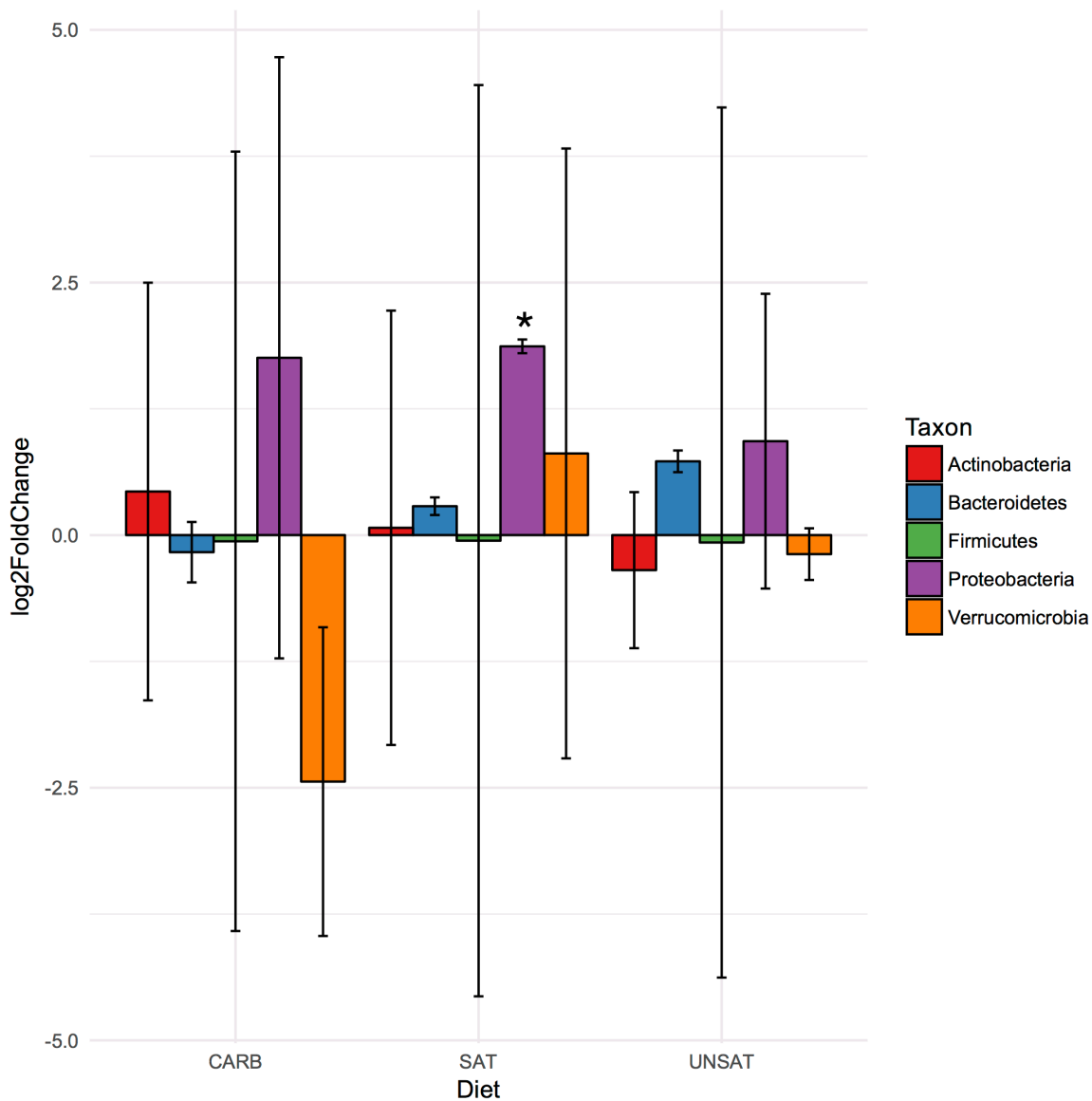**Figure S5. Microbiota composition in the study subjects at baseline.**

Figure S6. Mean log₂ fold-changes (± standard error) of the bacterial phyla in the groups. The fold-changes and their statistical significance before and after overfeeding are based on negative binomial models. Significant difference is indicated by the asterisk (p<0.05).

Table S1. Dietary profiles of the groups before and after the overfeeding based on food records.

	SAT (n=14)		UNSAT (n=12)		CARB (n=12)	
	Before	After	Before	After	Before	After
Energy intake (MJ/day)	7.61 (6.02 – 9.18)	11.67 (9.87 – 13.41)*	8.88 (7.99 – 10.89)	12.07 (11.05 – 13.54)*	8.20 (7.36 – 10.49)	12.15 (11.14 – 15.79)*
Protein intake (E%)	19.8 (15.2 – 21.7)	15.0 (11.5 – 15.5)*	18.8 (16.2 – 20.9)	13.2 (11.9 – 15.3)*	19.5 (16.1 – 22.0)	11.4 (9.4 – 14.5)*
Carbohydrate intake (E%)	38.4 (32.2 – 41.3)	25.9 (23.0 – 32.2)*	34.5 (31.6 – 39.7)	22.7 (19.3 – 28.9)*	40.0 (36.9 – 47.8)	63.7 (58.1 – 67.5)*
Fat intake (E%)	39.4 (36.5 – 42.1)	58.9 (53.1 – 61.1)*	38.8 (32.0 – 43.5)	59.7 (53.6 – 63.6)*	35.6 (31.5 – 42.4)	23.8 (19.6 – 25.8)*
Saturated fat intake (E%)	12.9 (11.7 – 14.6)	32.7 (27.6 – 35.5)*	12.9 (11.0 – 16.0)	14.3 (13.5 – 18.3)	13.1 (11.7 – 15.2)	8.3 (6.5 – 9.7)*
Monounsaturated fat intake (E%)	13.9 (11.9 – 16.8)	12.8 (11.9 – 14.9)	13.2 (11.2 – 15.9)	27.7 (23.1 – 30.4)*	12.1 (10.8 – 14.4)	8.5 (6.4 – 9.4)*
Polyunsaturated fat intake (E%)	6.7 (6.4 – 8.5)	4.5 (4.0 – 5.2)*	5.1 (4.9 – 9.2)	11.4 (9.5 – 13.5)*	5.6 (5.1 – 7.0)	3.4 (3.2 – 4.0)*

Data are in median (25th-75th percentile). No differences between groups at baseline (Kruskal-Wallis test). * p<0.05 in Wilcoxon Signed Rank test between Before and After within a group.

Table S2. Baseline fatty acid compositions of VLDL-TG according to groups.

Total	SAT (n=14)	UNSAT (n=12)	CARB (n=12)
C14:0 (%)	1.8 ± 0.2	2.0 ± 0.2	2.3 ± 0.2
C16:0 (%)	26.2 ± 1.0	27.0 ± 0.9	27.8 ± 0.8
C16:1 n-7 (%)	4.6 ± 0.5	4.4 ± 0.3	5.2 ± 0.5
C18:0 (%)	3.1 ± 0.3	3.3 ± 0.3	3.1 ± 0.3
C18:1 n-9 (%)	37.6 ± 0.9	37.8 ± 0.9	36.9 ± 0.9
C18:2 n-6 (%)	14.8 ± 1.0	13.7 ± 0.7	13.0 ± 0.9

Data are in means ± SEM. There were no significant differences in any variable between the groups.

Table S3. Plasma ceramide concentrations before and after overfeeding in the groups.

Lipid name	SAT Mean Before	Mean After	Q value	UNSAT Mean Before	Mean After	Q value	CARB Mean Before	Mean After	Q value
Cer(d16:2(4E,6E)/22:1(13Z)(2OH))	6.78643 +/- 0.96342	9.11274 +/- 1.33409	0.36	7.71353 +/- 0.87035	9.27031 +/- 1.25029	0.96	9.89585 +/- 1.71856	9.68906 +/- 1.3074	0.74
Cer(d18:0/24:0)	4.10406 +/- 0.38621	6.50034 +/- 0.57013	0.0052	3.99065 +/- 0.48144	4.35705 +/- 0.47258	0.97	4.52223 +/- 0.48002	4.28191 +/- 0.52112	0.88
Cer(d18:0/h24:0)	1.06967 +/- 0.06491	1.56036 +/- 0.09943	0.011	1.19847 +/- 0.08729	1.18781 +/- 0.103	0.99	1.36244 +/- 0.10395	1.32872 +/- 0.17257	0.72
Cer(d18:0/h26:0)	0.76885 +/- 0.0358	0.88989 +/- 0.09756	0.59	0.78448 +/- 0.04429	0.81856 +/- 0.07748	0.99	0.84401 +/- 0.05797	0.85801 +/- 0.09246	0.98
Cer(d18:1/24:0)	2.84316 +/- 0.31666	4.15985 +/- 0.34251	0.046	3.25284 +/- 0.35171	2.86855 +/- 0.39869	1	3.72058 +/- 0.40393	3.50024 +/- 0.48568	0.59
Cer(d18:1/24:1(15Z))	1.07751 +/- 0.10154	1.54825 +/- 0.14089	0.0026	1.27397 +/- 0.11128	1.25989 +/- 0.13142	0.96	1.37157 +/- 0.13407	1.16452 +/- 0.11646	0.59
Cer(d18:1/26:0)	2.07704 +/- 0.17362	3.1566 +/- 0.33601	0.53	2.45716 +/- 0.2555	2.53512 +/- 0.33441	0.97	2.40496 +/- 0.14202	2.15873 +/- 0.18681	0.72
Cer(d18:1/26:1(17Z))	0.45668 +/- 0.02678	0.59172 +/- 0.07791	0.29	0.46159 +/- 0.03213	0.50701 +/- 0.05571	0.97	0.54902 +/- 0.04149	0.52781 +/- 0.04814	0.7
Cer(d18:2/23:0)	0.86491 +/- 0.10664	1.31764 +/- 0.09732	0.0076	1.08901 +/- 0.10233	1.09294 +/- 0.12264	0.99	1.28808 +/- 0.18622	1.1395 +/- 0.1233	0.83
Cer(m18:0/24:0)	1.28955 +/- 0.18757	2.09629 +/- 0.21783	0.0018	1.43542 +/- 0.24432	1.46197 +/- 0.20338	0.99	1.61955 +/- 0.14476	1.56872 +/- 0.17573	0.93
Cer(m18:1(4E)/24:0)	1.02325 +/- 0.12517	1.60998 +/- 0.1801	0.034	1.25439 +/- 0.22107	1.27772 +/- 0.20404	0.99	1.38289 +/- 0.1927	1.4231 +/- 0.19509	0.92
Cer(m18:1(4E)/24:1(15Z))	1.96867 +/- 0.13806	2.60291 +/- 0.17806	0.011	1.99667 +/- 0.21621	1.89242 +/- 0.16879	0.97	2.96021 +/- 0.46321	2.20154 +/- 0.2227	0.7
Cer(m18:1(4E)/26:1(17Z))	2.69515 +/- 0.29105	4.29115 +/- 0.37047	0.02	3.31751 +/- 0.42431	3.34588 +/- 0.42823	0.97	3.42067 +/- 0.24066	3.05406 +/- 0.29993	0.72